Laser Photonics Rev. **6**, No. 5, 607–621 (2012) / **DOI** 10.1002/lpor.201100031

LASER & PHOTONICS REVIEWS

Abstract Non-Gaussian beam profiles such as Bessel or annular beams enable novel approaches to modifying materials through laser-based processing. In this review paper, properties, generation methods and emerging applications for non-conventional beam shapes are discussed, including Bessel, annular, and vortex beams. These intensity profiles have important implications in a number of technologically relevant areas including deep-hole drilling, photopolymerization and nanopatterning, and introduce a new dimension for materials optimization and fundamental studies of laser-matter interactions.

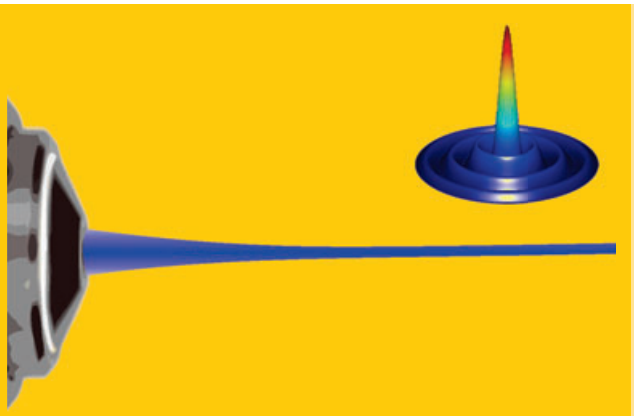

REVIEW ARTICLE

Bessel and annular beams for materials processing

Marti Duocastella and Craig B. Arnold*

1. Introduction

1.1. General laser processing

Lasers have become indispensible for materials processing in scientific and industrial applications. They offer a highly directional and localized source of energy, which facilitates materials modifications at precise locations [1]. Modern laser systems are also flexible, in the sense that it is relatively easy to adapt parameters such as the beam size or the beam energy to specific requirements, and systems can be scaled up to provide high throughput processing over multiple length scales [2].

The typical laser parameters that are controlled for materials processing include energy, fluence (energy per unit area), spot size, wavelength, polarization and, in the case of pulsed lasers, pulse duration and repetition rate [3, 4]. The role of these parameters on the resulting structures and properties has been widely studied, both experimentally and theoretically [3, 5, 6] and such understanding is essential in order to determine the optimum processing conditions. For example, laser fluence can affect the grain size of polycrystalline silicon (poly-Si) obtained through laser annealing of amorphous silicon. This factor can drastically influence the performance of poly-Si devices such as thin film transitors [7]. The response of biological tissues is dependent upon the laser wavelength, affecting the performance of surgical techniques such as Laser In Situ Keratomileusis (LASIK) [8]. Beam polarization can influence absorption in a given material [9], affecting the resultant structures achieved through techniques such as laser cutting or welding [10]. The rate at which energy is delivered in a material also affects the modification process [11]. In particular, the laser pulse duration can have a significant effect on the material removal dynamics. This leads to a more rapid ejection of material with a smaller heat affected zone as the temporal pulse length is shortened [12].

The control and influence of other laser parameters is less common yet these can also be important factors in materials processing. One of these is the laser beam shape, defined as the irradiance distribution of the light when it arrives at the material of interest [13]. Although some laser systems emit a multimode beam with a complex intensity distribution, most commercial lasers provide either a Gaussian intensity profile (Fig. 1a), a "Top-hat" intensity profile (Fig. 1b), or are modified to fall into one of these two categories.

1.2. Gaussian and Top-hat beams

Gaussian beams are by far the most common beam shape used in materials processing. Notably, the Fourier transform remains a Gaussian and thus preserves its shape as it passes through an optical system consisting of simple lenses. This is especially important in laser processing, where multiple optical elements are typically employed to guide the laser radiation to the workpiece.

Most lasers operate in the fundamental transverse electromagnetic mode of the cavity (TEM_{00}), and additional elements are not needed to modify the beam shape. Since the output of a finite cavity will have some non-ideal character, a quality factor M^2 ($M^2 \geqslant 1$) is defined which indicates how close a real beam is to a perfect Gaussian beam (M^2=1). Typical scientific, solid state laser systems have M^2 less than 2, however, industrial lasers with M^2 less than 10 are

Department of Mechanical and Aerospace Engineering, Princeton University, Princeton, New Jersey 08544, USA
* Corresponding author: e-mail: cbarnold@princeton.edu

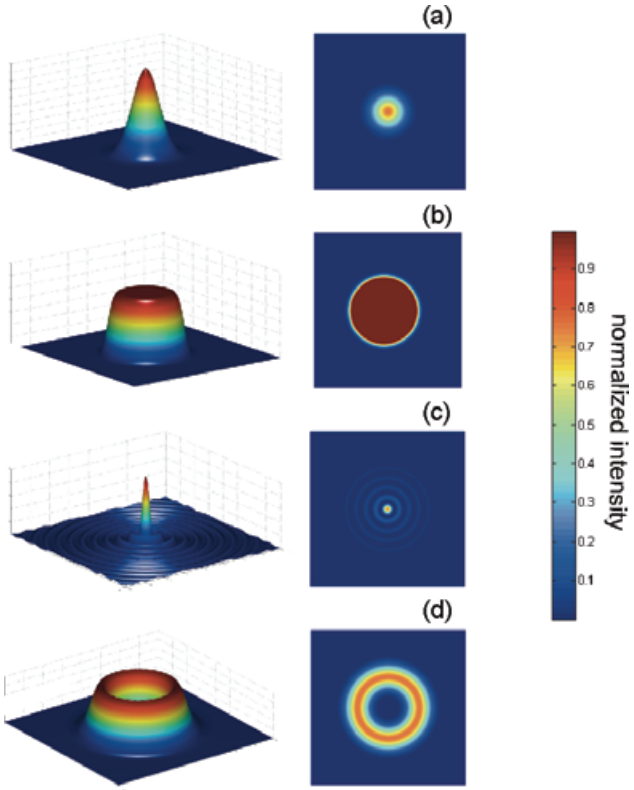

Figure 1 (online color at: www.lpr-journal.org) 2- and 3D intensity distributions of: (a) Gaussian beam; (b) Top-hat beam; (c) Bessel beam; (d) annular or doughnut beam.

still considered to be high quality Gaussian sources [14]. A common approach to improving the beam quality is to employ spatial filters [15]. However, for laser processing, the use of a pinhole is less desirable as it reduces the available energy, requires precise alignment, and can be damaged by high laser intensities.

An important property of Gaussian beams for materials processing is their low divergence, which allows for a small focused spot [16]. In fact, when focusing a Gaussian beam in air using a lens with a given numerical aperture NA the beam diameter at the focus (d_f) can be expressed, as [1]:

$$d_f \approx 2\frac{\lambda}{\pi}\frac{M^2}{\mathrm{NA}} \tag{1}$$

where λ is the wavelength of the laser radiation and we have assumed that the beam fills the lens aperture (1/e criterion). Therefore, Gaussian beams with M^2 close to 1 allow for a minimal spot size and thus enable a higher resolution than other, higher mode beams. According to Eq. (1), for a perfect Gaussian beam with a wavelength of 1064 nm (commercial Nd:YAG laser) focused through an objective with a NA of 0.5, one can achieve a focal spot size as small as 1.4 µm. This makes Gaussian beams ideal for microfabrication applications.

Another important factor in the laser processing of materials related to beam divergence, is the depth of field (z_f). In the context of materials processing, we can think of it as the distance a workpiece can be moved away from the beam waist while still maintaining the focal beam size. More specifically, it can be defined as the Rayleigh range, z_r [17]:

$$z_f = z_r \approx \frac{\pi}{4\lambda}\frac{d_f^2}{M^2}. \tag{2}$$

z_r represents the distance from the beam waist along the propagation direction at which the beam doubles its cross sectional area. For a 1064 nm laser with a Gaussian beam shape focused to a spot of 1.4 µm, the depth of field would be approximately 1.4 µm. Compared to other cavity beam modes, low M^2 beam have a relatively large depth of field, but under strong focusing conditions, the depth of field can still be too short for many industrially important processing applications.

Top-hat beams are also widely used for materials processing applications. For instance, excimer lasers generally produce a Top-hat output with varying degrees of uniformity across the beam. Alternatively, optical elements are used such as beam shapers when the output beam from the laser cavity is a Gaussian or homogenizer systems when the output is multimode. In comparison to Gaussians, Top-hat beams have an M^2 value much higher than 10. Thus, from Eqs. 1 and 2 it can be deduced that the minimum spot size will not be as small as with Gaussian beams, and that the depth of field will not be as long. However, the improved spatial uniformity of Top-hat beams present important benefits for specific materials processing applications in comparison to Gaussian beams [18]. This accounts for the preference of this type of beam for heat treatments such as laser annealing [19], materials deposition such as in pulsed laser deposition [20], welding applications with improved weld quality and repeatability [21], and even photolithography [22].

One of the major challenges associated with Top-hat beams is that unlike Gaussians, they do not maintain their shape as they propagate, and thus they only present a uniform intensity distribution near the focal point or imaging location of the optical system. Outside this zone, the beam profile and quality vary, which can lead to nonuniform processing and undesired effects.

1.3. Need for other beam shapes

Non-conventional beam shapes have the advantage that they can be explicitly designed to meet the requirements of a given material configuration or application that could not be feasible with either Gaussian or Top-hat beams. An example can be found in the use of photomasks for large array hole drilling for thin film transistor displays [23]. The photomask shapes a Top-hat beam into an array of beamlets, each with a uniform intensity distribution. Due to its parallel nature, this method reduces the processing time, and the uniform intensity distribution of each spot creates features with sharp edges. Beam shaping can also be an advantage in laser direct writing techniques such as laser-induced forward transfer (LIFT). In this technique, laser pulses are used to deposit volumetric pixels of material (voxels) from a donor film to

a receiver substrate [24]. Traditionally, LIFT is performed with Gaussian [25] or Top-hat beams [26] that enables the fabrication of patterns through the successive deposition of voxels with computer controlled positioning accuracy. However, recently, it has been demonstrated that one can deposit voxels with the specific shape of the incident beam [27]. In this way, complex patterns can be directly printed by arbitrarily shaping the beam, reducing the processing time and enabling high-throughput parallelization.

The possibilities that laser beam shaping offers are not limited to the previous examples, nor the field of materials processing. In fact, different beam shapes have been successfully used in several areas. For instance, the use of non-conventional beam shapes in optical manipulation, such as Bessel beams [28, 29] or Airy beams [30], has allowed the simultaneous trapping of several particles at the same time or the transport of 60 µm microspheres over a distance of half a meter. Such performance is not possible with either Gaussian or Top-hat beam shapes. In atom optics, Laguerre-Gaussian or optical vortex light beams have been successfully used for atom guiding [31–33], and it has been demonstrated that Bessel beams can produce elongated atom traps not achievable with Gaussian beams [34]. The use of annular beams combined with Gaussian beams has enabled novel imaging techniques such as stimulated emission depletion (STED) microscopy [35, 36]. Finally, for novel applications in biology such as cell transfection through optoinjection, the use of Bessel beams obviates the need for accurate focusing on the soft cell membrane, thus making the overall process more efficient [37, 38].

One of the things to keep in mind with structured beams for materials processing is that most methods of shaping the beam inevitably reduce the amount of energy available for modification. In this respect, Gaussian beams have an advantage over any other beam shape as discussed above. However, the trade-off of reduced power associated with shaped beams may be more appropriate in certain cases, due to the unique material responses that they can generate. Therefore, beam shaping can be considered an important controlling parameter in the pursuit of process optimization, as well as a viable approach to increase the flexibility of lasers, expanding their use in new and interesting directions.

1.4. Statement of paper direction

This present paper reviews emerging applications of Bessel and annular beams in materials processing. These two beams are closely related through their Fourier transform and exhibit unique properties that open the door to numerous opportunities in research and industrial applications. Such properties are discussed along with an analysis of the advantages and disadvantages these intensity profiles present. In the first section of this review, the properties and the methods to generate these beams are presented. Next, we review recent work in materials processing for which Bessel and annular beams are employed. Finally, we conclude with a discussion of the future outlook for Bessel and annular beams laser processing.

2. Bessel and annular beams

For the purposes of this paper, we define a Bessel beam to mean a beam whose electric field is explicitly described by a zeroth-order Bessel function of the first kind (J_0):

$$E(r,\varphi,z) = A_0 \exp(ik_z z) J_0(k_r r) \tag{3}$$

where r and φ are transverse and polar coordinates, z is the coordinate in the propagation direction, and k_z and $k_r$are the longitudinal and radial wavectors. More generally, the term Bessel beam could refer to higher order functions although we ignore those here. Since the beam intensity is proportional to the square of the electric field for a Bessel beam,

$$I(r,\varphi,z) \propto J_0^2(k_r r)\,, \tag{4}$$

this beam does not appear as a single spot, but rather as a series of concentric rings (Fig. 1c). Another way to think about a Bessel beam and its "bulls-eye" pattern, is to consider its formation as the result of the interference of plane waves with wave vectors belonging to a conical surface. A region of self-interference develops in which the Bessel pattern emerges due to cylindrical symmetry. It should also be pointed out that, according to Eq. (4), the number of rings of a Bessel beam should be infinite. However, in laboratory generated Bessel beams the presence of finite apertures produces Bessel beams with finite dimensions. In the present paper only these 'finite Bessel beams', also referred to as quasi-Bessel beams [39], will be considered. It is important to note that in the far field, as the separation between the wavevectors increases, the beam intensity in the central axis decreases and eventually attains a null value, which corresponds to an annular beam.

An annular beam, also called doughnut-shaped beam, is a beam with an intensity distribution concentrated in a ring with no on-axis intensity, as represented in Fig. 1d. There exist multiple sorts of annular beams depending on the irradiance distribution within the annulus. For instance, the distribution can be constant in r and θ, in which case the annular beam is described by the equation:

$$I(r,\theta) = \begin{cases} I_0 & r_i \leqslant r \leqslant r_o \\ 0 & \text{rest of points} \end{cases} \tag{5}$$

where I_0 is the intensity within the annulus, r and θ are the polar coordinates, and r_i and r_o the input and output beam radii, respectively. More commonly, annuli with a Gaussian profile in the r direction are generated. The equation that describes such beams is:

$$I(r,\theta) = I_0 \exp\left(-2\frac{(r-r_c)^2}{\omega^2}\right) \tag{6}$$

where I_0 is the maximum intensity of the beam, r_c is the position of I_0, and ω is the beam waist. An annular beam can also be formed by subtracting two Gaussian beams of the same maximum intensity but with different beam waists. In this case, the resulting beam intensity would be:

$$I(r,\theta) = I_0\left[\exp\left(-\frac{2r^2}{\omega_1^2}\right) - \exp\left(-\frac{2r^2}{\omega_2^2}\right)\right] \tag{7}$$

where, ω_1 and ω_2 correspond to beam waists of the two Gaussian beams.

A related structure to the annular beam is the so-called optical vortex (OV) beam. The discovery that a beam of light with a well-defined orbital angular momentum can be created rather easily in a laboratory [40] opened up the possibility to study the role of this new optical parameter in light-matter interactions [41]. An OV beam takes advantage of this property and is defined as a beam whose phase varies azimuthally along the direction of propagation. OV's are characterized by their topological charge (m), which corresponds to the number of twists in the phase front within one wavelength. Due to the twisting of the phase front, the phase in the beam center is multiply defined, giving rise to an optical singularity that produces a vanishing amplitude at this point [42] giving the appearance of an annulus in intensity.

It is important to note that the literature tends to take a general view to the term "annular beam" and uses it to refer to any beam with a null intensity along the beam axis such as OV beams. For instance, first order Bessel beams [43], whose intensity is proportional to the square of a first order Bessel function (J_1), or higher order Laguerre-Gauss modes [44] fall into this category. Such different annular beams can lead to unique material responses [45] and therefore one must use care in distinguishing experiments employing this general class of intensity profile.

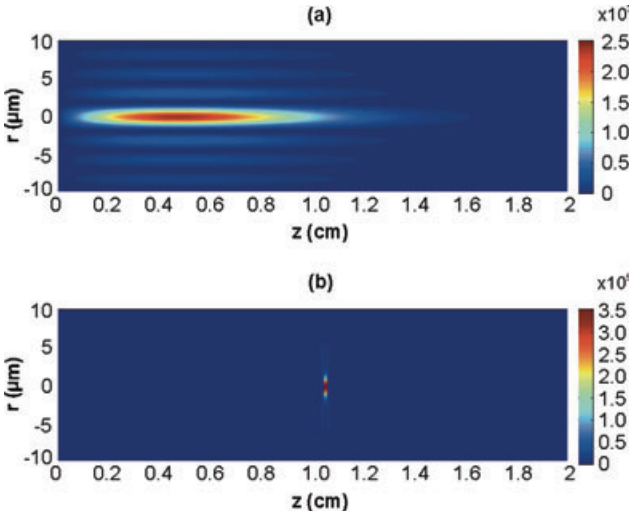

Figure 2 (online color at: www.lpr-journal.org) Simulations of the intensity distribution along the propagation distance z from the focusing objective of: (a) a Bessel beam generated using an axicon (wedge angle of 12°) to focus a Gaussian beam (532 nm, ω_0=1 mm) (b) same Gaussian beam focused using a microscope objective (NA of 0.25). Although the central lobe of the Bessel beam and the Gaussian beam have the similar radial dimensions, their differences are evident: the Bessel beam exhibits a longer depth of field, whereas the maximum intensity of the Gaussian beam in the focal region is higher.

2.1. Properties of Bessel and annular beams

A detailed description of the properties of Bessel beams can be found in [34] and [39]. Perhaps the most important optical property for materials processing is the extended depth of field of Bessel beams. This 'nondiffracting' effect occurs as a result of minimal spreading in the central lobe during wave propagation [46, 47]. Such behavior is illustrated in Fig. 2, in which an incident Gaussian beam either propagates through a converging lens to its focus, or is shaped into a Bessel beam. The elements are selected such that the beam waist of the Gaussian is the same as the width of the central lobe of the Bessel beam (Fig. 2a). Although the maximum intensity along the principle axis is lower in the case of the Bessel beam, the FWHM along the z-direction is orders of magnitude greater (1 cm vs 0.01 cm).

In fact, the Rayleigh range for a Bessel beam can be approximated as:

$$z_{\text{Bessel}} \approx \frac{\pi D d_f}{4\lambda} \tag{8}$$

where D is the diameter of the aperture, d_f the diameter of the central lobe, and λ the laser wavelength [48]. Comparing Eq. (8) with the corresponding Rayleigh range of a Gaussian beam (Eq. (2)), it can be observed that Bessel beams have a much larger Rayleigh range when $D \gg d_f$, as it is usually the case. Thus, Bessel beams exhibit a greater depth of field than Gaussian beams. The cost of this increased depth of field is that optical energy is distributed among the rings in the pattern and so the nondiffracting property of a Bessel beam comes at the expenses of power and contrast [46]. However, as we will see below, the benefits of high-depth of field for applications such as deep hole drilling or manufacturing on uneven surfaces outweighs these trade-offs.

A second optical property of Bessel beams that is their ability to reconstruct after an obstruction [28], in an effect that is commonly called 'self-healing'. This can be understood by considering the construction of a Bessel beam as a superposition of plane waves propagating on a cone. In this way, if an obstacle is placed in the center of the beam, it will block some of the rays, but others will interfere again after the obstruction and reform the beam. This unique property can help to mitigate effects of debris and other products of the laser processing that can partially block incident beams. With conventional beams, such blocking can result in processing nonuniformities.

In the case of annular beams, the null intensity on-axis has important implications for thermal and mechanical effects in materials [49, 50]. This is demonstrated in Fig. 3, where we simulate the temperature profiles of silicon after 333 μs of irradiation with a CW laser with a Gaussian beam (beam waist 800 μm), a Top-hat beam (diameter of 800 μm) and with an annular beam (exterior beam diameter 800 μm). The Gaussian beam produces a temperature increase mainly in an area localized by the beam waist. The same occurs with a Top-hat beam, although the lateral extent of the heated area is greater. When using an annular beam, the lateral spreading of the heated area is still larger while the maximum temperature rise is lower in the center.

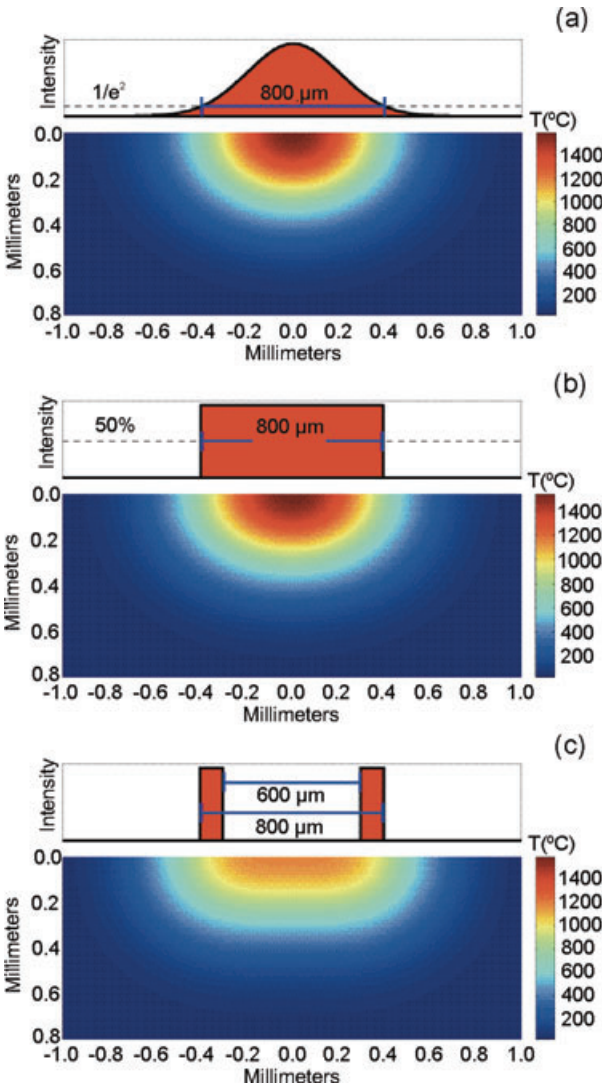

Figure 3 (online color at: www.lpr-journal.org) Simulations of the temperature profiles in silicon at 333 μs after depositing 1 J of energy, assuming an absorption depth of 1 μm for: (a) Gaussian beam; (b) Top-hat beam; and (c) annular beam. (Thanks to Matthew Brown for generating this figure.)

These differences in the temperature profiles are crucial for applications in which temperature is a key parameter, such as laser heat treatment or laser hardening. It is also worth mentioning that when a material is irradiated with a CW laser beam with an annular shape, the induced stress in the center of the irradiated area is minimal [51], a phenomenon that does not occur with other beam shapes, and one that can be employed in processes such as glass cutting for which controlling stress is desired.

2.2. How to generate Bessel and annular beams

2.2.1. Aperture based methods

Bessel and annular beams can be generated using apertures. In fact, the first experimental realization of a Bessel beam

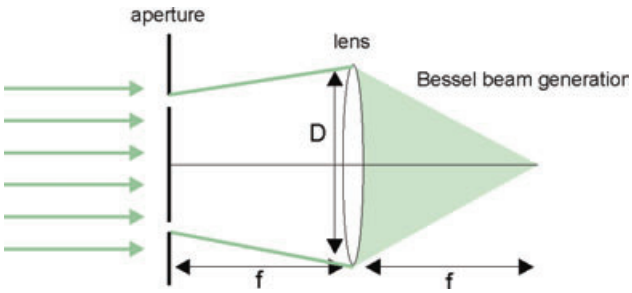

Figure 4 (online color at: www.lpr-journal.org) A plane wave is used to illuminate an annular aperture situated in the back focal plane of a convergent lens. As a result, a Bessel beam is formed in the image plane [48].

was achieved using this method [48], an annular slit was situated in the back focal plane of a convergent lens and was illuminated with a plane wave (Fig. 4). The electric field at the aperture plane can be written as:

$$E_{\text{slit}} = A_i \delta (r - r_s) \tag{9}$$

where A_i is the wave amplitude, δ is the Dirac delta function, and r_s the slit diameter. The electric field at the front focal plane of the lens is proportional to the Fourier transform of the incident electric field [52]. Due to the circular symmetry of the system, this Fourier transform can be written as a Fourier-Bessel transform,

$$E_{\text{front}}(r) = \frac{2\pi}{i\lambda f} \int_0^\infty r' E_{\text{slit}}(r') J_0(2\pi r' \rho)\, dr' \tag{10}$$

where the Fresnel diffraction formula has been employed, and $\rho = r/\lambda f$, with λ being the plane wave wavelength and f the lens focal distance. The solution of Eq. (10) is:

$$E_{\text{front}}(r) = A_i \frac{2\pi r_s}{i\lambda f} J_0\left(\frac{2\pi r_s r}{\lambda f}\right) \tag{11}$$

which has the same form as Eq. (3), the definition of a Bessel beam.

Although successful in generating a Bessel beam, this method, is highly inefficient since the aperture blocks most of the incident radiation. This reduction in the available energy is unsuitable for applications where high intensities are needed. Thus, for materials processing applications, other methods are generally more desirable.

Annular beams can also be generated using apertures. Apart from the annular beam encountered in the far field of any finite Bessel beam, the introduction of an additional lens in the previous setup also allows the generation of annular beam. The lens will produce the Fourier transform of a Bessel beam, which is an annular beam. Again, the low throughput of this configuration is not favorable for materials processing.

2.2.2. Axicons

An axicon, or conical lens element, as shown in Fig. 5 is perhaps the most convenient and cost-effective way to generate a Bessel beam [53]. In this case, the incident beam

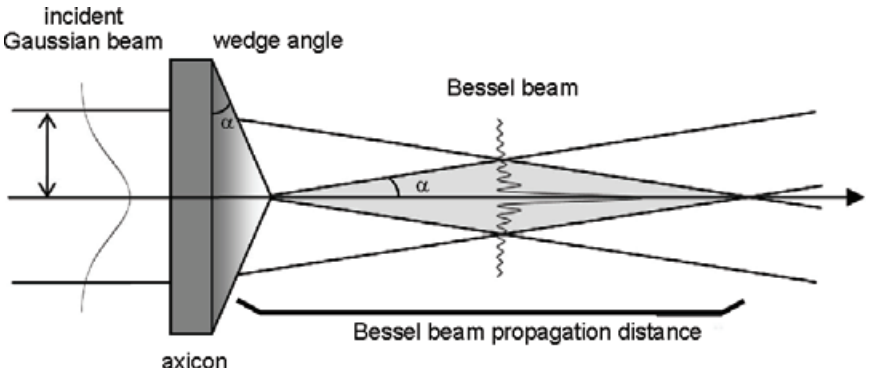

Figure 5 Creation of a Bessel beam using an axicon illuminated with a Gaussian beam. If a convergent lens is placed after the axicon, an annular beam is produced in the lens focal plane.

is refracted in order to produce the interference pattern described earlier. This approach provides a more optically efficient way to produce a Bessel beam than aperture-based methods. However, the alignment between the incident laser beam and the axicon is a critical issue, which can result in nonuniformities if not properly aligned [31]. Usually, the incident beam is Gaussian, in which case the resulting beam after the axicon is called Gaussian-Bessel, and its intensity profile is [54, 55]:

$$I(r,z) = 2k\pi\left(\tan^2\alpha\right)(n-1)^2 z I_0 e^{-2(n-1)z\tan\alpha/\omega_0} \times J_0^2(kr(n-1)\tan\alpha) \quad (12)$$

where r and z are the radial and longitudinal coordinates, I_0 and ω_0 are the intensity and beam waist of the incident Gaussian beam, k is the wave vector, n the index of refraction of the axicon material, and α is the wedge angle. This equation can be equivalently written in terms of the cone angle β at the tip of the axicon. Using Eq. (12) one can determine the width of the central lobe by finding the first zero of the Bessel function. This yields,

$$d_f = \frac{2.4a}{k(n-1)\tan(\alpha)} \quad (13)$$

where a is a constant of order unity. Substituting this into Eq. (8) for the Rayleigh range gives

$$z_r \approx \frac{D}{2(n-1)\tan(\alpha)}. \quad (14)$$

Therefore, the wedge angle of an axicon ultimately determines the waist and extent of the central lobe of the Bessel beam [56], with smaller angles corresponding to wider lobes and longer "diffractionless" propagation. For typically implementations in materials processing, this wedge angle is small (< 0.1 rad).

Annular beams can also be formed with an axicon in two different ways. The first one is to simply place the workpiece at a distance far enough from the axicon in order to encounter the far-field profile of the axicon which corresponds to an annulus. Alternatively, one can combine the axicon with another focusing element to create an annulus at the focal plane of the system [57]. The outer diameter of the annulus generated in this way is given by:

$$d = 2F\tan\left(\alpha\left(n-1\right)\right) \quad (15)$$

where F is the effective focal length of the lens [58]. This latter approach enables greater control over the size and shape of the annular beam.

Axicons can be either refractive or diffractive with the former ones being widely adopted due to the relative simplicity of fabricating them. Recently, researchers have shown the ability to produce a fluid based tunable device that allows one to control the wedge angle of the axicon [59]. Diffractive axicons are similar in construction to Fresnel lenses, and have the advantage of being thinner than refractive axicons. Additionally, for ultrashort pulses commonly encountered in materials processing, beams created by diffractive methods are less likely to suffer broadening due to non-linear characteristics of the lens material [60].

2.2.3. SLM based methods

A spatial light modulator (SLM) is a digital device that modifies the phase and/or intensity of an incoming laser beam. These devices have become popular for their ability to produce arbitrary beam profiles and holograms for wide-spread applications in processing and imaging [61, 62]. One can easily produce a phase pattern in an SLM that corresponds to a diffractive axicon, and as a result, the SLM will generate Bessel or annular beams with user-defined wedge angles [63]. It is also possible to imprint a helical ramp phase with a central singularity [64], which allows the direct formation of an optical vortex beam. There are different types of SLMs, such as magneto-optic SLMs [65], deformable mirror SLMs [5], or liquid crystal (LC) SLMs [66]. Although providing the widest range of intensity profiles, these devices tend to have relatively low damage thresholds limiting their applicability in materials processing to low average power processes. The incorporation of a cooling system can help increase the damage threshold and has enabled the use of higher powered nanosecond lasers for micromachining using SLMs [67].

2.2.4. TAG lens

A tunable acoustic gradient (TAG) lens provides an alternative adaptive optical method of creating a user-defined Bessel or annular beam. In the TAG an acoustic field is

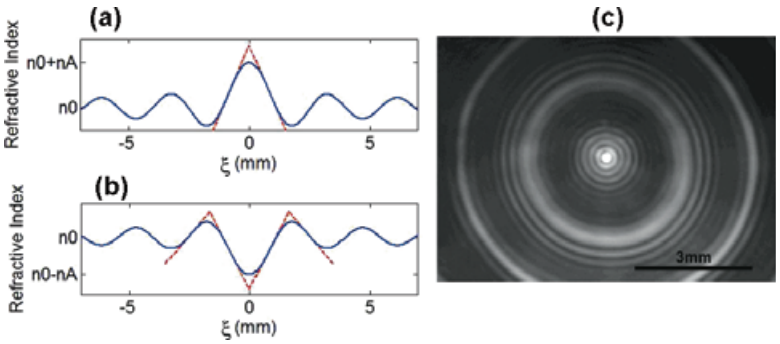

Figure 6 (a) Index profile of the TAG lens at one instant in time and (b) half-period later in time. (c) Multiscale Bessel beam created by the TAG lens. The TAG lens is driven at a frequency of 257 kHz, and a CW green laser is used for illumination [72].

generated in a liquid chamber leading to a periodically varying index of refraction profile in the device [68–71]. When using a cylindrical chamber, this index can be written as

$$n(r,t) = n_0 + n_A J_0\left(\frac{\omega r}{v}\right)\cos(\omega t) \qquad (16)$$

where n_0 corresponds to the static refractive index, ω to the driving frequency, v to the speed of sound in the fluid, and n_A is a constant that depends on the physical properties of the medium and the driving voltage amplitude (Fig. 6a,b). When light passes through this index of refraction profile, it is transformed into a multiscale Bessel beam [68] where a central Bessel beam is formed surrounded by additional Bessel-like rings (Fig. 6c) [72]. The particular output pattern of the TAG lens can be selected by synchronizing a pulsed laser with the phase of operation of the TAG. Under the appropriate conditions, it can provide a simple Bessel or annular beam to be used for materials processing or imaging [73–75]. The properties of the TAG generated beam can be modified by varying the frequency and/or amplitude of the lens driving signal. These parameters can be rapidly changed and as such, the switching time of the TAG lens is on the order of microseconds [76], which makes it significantly faster than commercial SLMs.

2.2.5. Optical fibers

Optical fibers have been recently reported as a valid alternative for the generation of Bessel or annular beams. The main advantage of optical fibers compared with the previous methods is the lack of free-space elements, which facilitates integration in miniaturized systems. Moreover, they have an added benefit in their inherent compatibility with the rapid developing fiber lasers for materials processing applications [77].

There exist multiple approaches to generate Bessel beams using optical fibers. For instance, one can fabricate an axicon on the tip of a fiber using chemical etching methods [78,79] or by appropriately polishing the fiber tip [80]. A Bessel beam can also be obtained by using a hollow optical fiber with a polymer converging lens in its tip, in an analogous way to the aperture method described in 2.2.1 [81]. The use of multimode (MM) fibers provides a different approach to generate higher-order Bessel-like beams. In MM fibers the excited modes, represented as $LP_{0,n}$ (n being the radial index) correspond to zeroth order Bessel functions. Thus, the propagation of light in MM fibers produces interferences between different fiber modes that result in a Bessel-like beam with non-diffracting characteristics [82, 83]. Alternatively, it is possible to design a fiber that selects a single high-order fiber mode ($LP_{0,n}, n>5$), which is accomplished using long period fiber gratings [84, 85]. This approach offers a high conversion efficiency and allows the formation of beams with a high similarity to ideal Bessel beams [86].

Annular beams can be generated using any of the fiber-based approaches mentioned above at the far-field of the fiber output. In addition, there exist inherent annular beam generation methods using optical fibers. For instance, a fiber with a small hollow in its center produces these beams [87]. It is also possible to obtain an annular beam at the output of a MM fiber (with a parabolic refractive index) illuminated with an input beam that presents a certain incidence angle with respect to the fiber axis [88, 89]. The requirement of such tilting, though, reduces the coupling efficiency and the output power, which can be detrimental for laser processing applications.

2.2.6. Other methods

In addition to the more common methods mentioned above for materials processing, there are a number of alternative ways to obtain Bessel or annular beams. Researchers have found success using pre-fabricated holographic displays [90], diffractive optical elements [12, 91], optical phase plates or spatial phase masks [92]. For OV beams, spiral phase plates (SPP), a dielectric material with a thickness that varies azimuthally around the plate have shown great potential for high-intensity beam propagation [93]. In addition, uniaxial birefringent crystals [94], have allowed the successful generation of high-intensity ultrafast vortex pulses without broadening, thereby providing a convenient tool to study material processing with OVs.

3. Applications of annular and Bessel beams for materials processing

Annular and Bessel beams enable unique material responses, which offer new fundamental insights in light-matter interactions and have the potential to extend the possibilities of

laser processing. In this section, we review recent works in laser processing areas where these beams are providing a novel and unique alternative to traditional beam shapes.

3.1. Microdrilling

Laser drilling of micron-sized holes is a well-established industrial process used in a number of applications ranging from car manufacturing to consumer electronics [95]. Laser fluences above the ablation threshold lead to direct material removal and the formation of a hole. The quality of the hole depends on both the properties of the irradiated material as well as the laser processing parameters. Despite the widespread industrial use of lasers as drilling tools, research to optimize the system performance such as speed, throughput, sidewall taper, or symmetry remains actively pursued. The laser parameters such as the wavelength or pulse duration are well known to affect such things as the hole diameter, the taper, or the thermal effects beyond the irradiated area [3, 16]. In addition, the laser beam shape also plays a crucial role in determining the hole quality. For instance, drilling with a Top-hat beam produces sharper edges than similar processing with a Gaussian beam which can produce tapered holes [96].

Drilling with annular beam shapes can also be advantageous. For instance, drilling holes with diameters larger than the beam typically requires trepanning, a method in which the laser beam is scanned in a circularly-closed pattern to create the hole [45]. This process requires moving the part or the optical system with high speed and precision. In contrast, an annular beam successively fired on the same region in a percussion drilling manner performs the analogous process. This approach which has been referred to as optical trepanning, has successfully been used to drill submillimeter-size through-holes on stainless steel [97]. In that work, an axicon was used to generate an annular beam, which was later collimated with a second axicon and finally focused on the sample through a converging lens as described earlier by Rioux [57]. Controlling the relative distances between the axicons and the lens makes it possible to vary the dimensions of the annular beam and consequently the dimensions of the resulting hole. The main complication of this approach is that the alignment between the incident laser beam and the two axicons is critical and any misalignment can easily result in nonuniformities and inefficient hole drilling. A possible solution to this problem is to use a TAG lens device [68, 70] to generate the annular beam. Such device is easy to align, and it has the added advantage of quickly switching between different beam shapes. This device has been employed to drill annular blind-holes on a polyamide film [98].

A Bessel beam can also offer advantages when drilling micron-sized holes on structured, rough, or uneven substrates or when the substrate is non-planar. To drill such holes with conventional beams, a high numerical aperture lens creates a tight focus, which implies a short depth of field (Eq. (2)). Thus, in order to obtain holes of the same size on surfaces at different heights, the position of the beam must be adapted to the substrate irregularities so that the working distance is preserved. This can be solved by setting up a laser-position monitor and motion control system, which add complexity and cost to the manufacturing process. An alternative way to solve this problem is to use a Bessel beam which can combine a narrow central lobe with a long depth of field. This increases the tolerance of the focal plane position during processing, allowing holes with the same characteristics over long distances. The feasibility of drilling such holes with a Bessel beam has been demonstrated for silicon [99], and for chromium [60]. In these works, blind-holes with a diameter below 10 µm were drilled using nanosecond laser pulses as a function of the distance away from the axicon. Researchers found that the hole morphology was maintained for changes in distances as large as 2 mm along the axial direction. The same approach with Bessel beams has been employed to drill holes on glass using femtosecond laser pulses [63]. In this case, uniform holes with a diameter of 500 nm were obtained for up to 20 µm differences in surface height.

A field in which Bessel beams can also be employed is in the simultaneous processing of large sample areas for industrial applications such as marking or data storage. Usually, parallel processing is accomplished by splitting a laser beam into an array of beamlets and focusing each of them onto the substrate of interest [16]. However, the formation of uniform patterns over large areas requires a precise alignment between beamlets and substrate. These alignment constraints can be overcome thanks to the long depth of field of Bessel beams. This has been demonstrated through the fabrication of periodic two-dimensional channels on poly(methyl methacrylate) using an array of refractive cylindrical axicons [100]. Moreover, placing a lens before the axicon arrays allowed varying the spacing between the channels by translating the substrate without compromising the characteristics of the channels.

Bessel beams have also been used to drill through-holes on different metal foils such as stainless steel [56, 99], and copper [55]. However, the adequacy of using these beams for such application is controversial, mainly for two reasons. The first one is the presence of a ring structure on the irradiated area, as illustrated in Fig. 7. Such rings extend over an area much larger than that of the hole, distributing energy away from the central region and possibly leading the formation of structure on the surface. It may be argued that such rings could be avoided selecting a Bessel beam with only the central lobe capable of reaching the intensity required to ablate a material or other high-order beam shapes [93]. However, in order to drill a through-hole on a metal, high fluences and a large number of pulses can be required. As a consequence, the accumulation of energy can cause ring marks on the irradiated area. The second aspect that potentially limits the use of Bessel beams for through-hole drilling in metal foils is blocking of the beam by the metal itself. As mentioned before, Bessel beams can be considered to be the result of the interference between plane waves. In the case of metals, since they are opaque such plane waves would not propagate inside the material, and thus the long depth of field of the Bessel beam would be

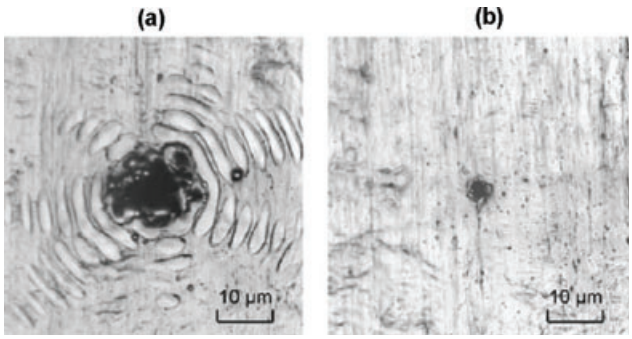

Figure 7 Scanning laser microscope images of a hole drilled using a Bessel beam into a stainless steel sheet with a thickness of 20 μm. (a) Irradiated surface, with the characteristic marks of left by the Bessel rings; (b) rear surface, with a hole smaller than at the entrance showing tapering [56].

lost. However, if the drilled metal foil is thin enough, holes drilled with a Bessel beam can exhibit sharper sidewalls and less taper than holes drilled into the same foil using a Top-hat or Gaussian beam [56].

3.2. Fabrication of micro/nano channels in transparent materials

Machining transparent materials with ultrashort laser pulses (shorter than 1 ps) has become a common process for producing structures within the volume of a material for optical and photonic applications as well as dicing and cutting [101]. Despite the apparent contradiction of using a laser to modify a material that is transparent to that laser wavelength, when ultrafast laser pulses are focused into small spots the intensities achieved in the focal volume are high enough to induce nonlinear absorption, modifying the material properties in that region [2]. Thus, the material modification is localized in 3D, whereas the rest of the material remains unaltered. Such spatial confinement, in addition to the translation of the laser within the material or other non-linear effects such as filamentation [102, 103], can be used to generate channels or complex three-dimensional structures.

The use of non-Gaussian beam shapes, with their unique properties, can be beneficial for machining transparent materials in many instances. A situation that illustrates this is the fabrication of long three-dimensional channels with a reduced diameter, which is important for applications such as microfluidics or for waveguide fabrication. Such channels are usually obtained with a Gaussian beam and a high NA lens to focus the radiation into a micron-sized spot combined with translation of the sample to produce the channel. This requires precise alignment and feedback, which further reduces the speed of the process. A Bessel beam introduces a more efficient way to produce such long channels. In this case, and contrary to what occurred for opaque materials, the plane waves that form the Bessel beam can propagate through the transparent material and provide the beam with a high depth of field within the bulk material. Due to the localization of multiphoton absorption to only the narrow central focus region, the Bessel beam can produce long channels while maintaining a small diameter.

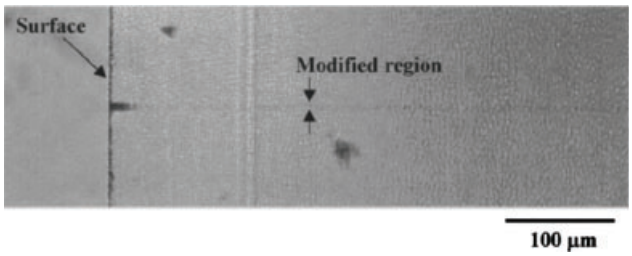

Figure 8 Photograph of the modification generated in a 3 mm thick glass using a Bessel beam. Several ultrashort laser pulses were employed to create the 5 μm thick channel [60, 105].

The feasibility of using Bessel beams to fabricate long, 3D structures was first demonstrated by *Marcinkevicius* et al [104]. In that work and in the subsequent ones [60, 105], the irradiation of silica led to modifications of the material along the beam path, as shown in Fig. 8. These changes in the index of refraction have been used to produce high-quality waveguides with low loss and without birefringence [106, 107]. Complete hollow 3D structures were latter fabricated on glass through a two step process: firstly the material was irradiated with the Bessel beam and afterwards it was exposed to a chemical etching process [60, 105]. However, the use of etching agents adds complexity and variability to the process, since the etching time has to be carefully controlled and the etching agent has to arrive to all the parts of the structure, which can be hard to control in 3D structures.

It has not been until recently that high quality glass microchannels have been fabricated without chemical etching using Bessel beams [108]. In this case, the intensity of the femtosecond laser pulses was high enough to induce filamentation and self-focusing. Filaments within transparent materials generated by Bessel beams had already been observed to reach long distances [109], and theoretical work predicted that the propagation of such filaments were more stable over longer distances than those generated by Gaussian beams [110]. The microchannels produced by filamentation had an aspect ratio as high as 40 without tapering. To obtain such taper free structures rear-side illumination with the sample immersed in water was carried out, which helped debris evacuation and the formation of well-defined structures. Nanochannels on glass have also been generated using the filamentary propagation of Bessel beams [111]. In this case, a single laser pulse was used to generate channels with a diameter of about 500 nm and lengths of the order of 50 μm (Fig. 9).

3.3. Micromachining using vortex beams

The first experiments on laser machining using OVs have appeared recently and showed promising results for efficient ablation and the ability to create unique material structures [112]. The morphology of holes ablated on a Tantalum surfaces using nanosecond OV pulses exhibited less debris

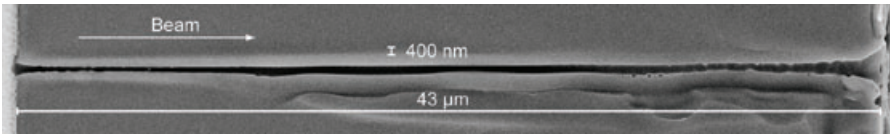

Figure 9 SEM image of a channel generated in glass using a single shot from a Bessel beam. The intensity of the femtosecond pulse was high enough to induce filamentation [111].

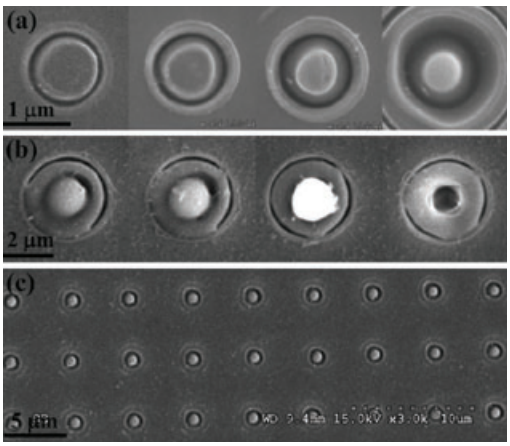

Figure 10 SEM images of ablation rings on soda-lime glass produced with single femtosecond vortex pulses. (a) Ablation energies of 100, 150, 250, and 700 nJ, from left to right. (b) Cavities on the beam axis, where the intensity is negligible, produced at an energy of about 1.5 µJ. (c) 200 µm x 200 µm array produced at an energy of 250 nJ, which demonstrates the reproducibility of the ablation process [50].

and a better definition than those processed using annular beams without orbital angular momentum (OAM). By using circularly polarized light in combination with the OV, it becomes possible to create microneedles in the central region of the ablated spot without affecting the surrounding material.

Femtosecond vortex pulses can also lead to the modification of material in the center of the annular intensity profile, as demonstrated by irradiating soda-lime glass [50]. Femtosecond OV pulses with fluences slightly above the ablation threshold resulted in reproducible annular holes with clean edges. As the fluence was increased, deep cavities started to form in the annulus center where the residual light was negligible (Fig. 10). The formation of these cavities has been attributed to a toroidal plasma induced by high-intensity vortex pulses [50]. The expansion of such torodial plasma produces two shock waves: one that propagates towards the surrounding material and one to the annulus center. This second one would produce a dramatic rise in pressure when reaching the annulus center and leads to material removal. Therefore, from the previous examples it can be concluded that OVs induce very particular light-matter interactions that could be advantageous in several laser processing applications.

3.4. Nanopatterning

The processing of materials on the nanoscale is a growing demand in several areas, including electronics [113] and biotechnology [114]. The diffraction limit of conventional focusing optics has traditionally restricted the use of optical techniques to micron and sub-micron size scales. However, recent strategies have been developed to overcome this limit. Apart from the previously mentioned multiphoton absorption, near-field effects can similarly overcome traditional diffraction limitations to produce nanoscale features [115]. This takes the advantage of evanescent waves near interfaces and surfaces, usually generated after irradiating a particle or near-field objective with a laser beam, to allow an enhancement of the electric field in a confined region close to the particle surface. Arrays of dielectric microbeads can be self-assembled on a surface [116, 117] and a single laser pulse can be used to create a corresponding array of isolated dots or other shapes [118–120].

However, in order to harness the near-field intensification of light for user defined nanopatterns, it is necessary to manipulate the near-field objective along the surface while accurately maintaining a separation of 10's of nm from the workpiece surface. It is possible to do this by taking advantage of the "nondiffracting" behavior of Bessel beams for optical trapping. Contrary to conventional optical traps using Gaussian beams, Bessel beam traps only exhibit significant gradients in the transverse directions, which leads to particle confinement in two dimensions with a scattering force in the propagation direction [121]. This scattering force can be balanced by the interaction forces between the particle and surface, such as Van der Waals, seteric and electrostatic repulsion, resulting in an equilibrium distance between particle and surface on the order of 50 nm depending on the trapping laser intensity and system chemistry [122]. Therefore, the use of Bessel beams enables the self-positioning of the particle relative to the substrate regardless of surface inhomogeneities and without the requirement of feedback control. As a consequence, if the trapped particle is irradiated with a second laser pulse so that the near-field effects induced enable the modification of the workpiece surface, it is possible to controllably generate nanofeatures. The feasibility of this technique, called optical trap assisted nanopatterning (OTAN), has been demonstrated through the creation of various types of surface modifications, including bumps, pits and holes, depending on the material and the pulsed laser fluence [121] (Fig. 11), the implementation of parallel nanopatterning [123], and even the ability to traverse rough and textured surfaces [124, 125]. The minimum feature sizes were 100 nm, and the positioning accuracy was better than 40 nm.

3.5. Photopolymerization

Photopolymerization using laser beams is a well known prototyping technique that can be used to fabricate micro

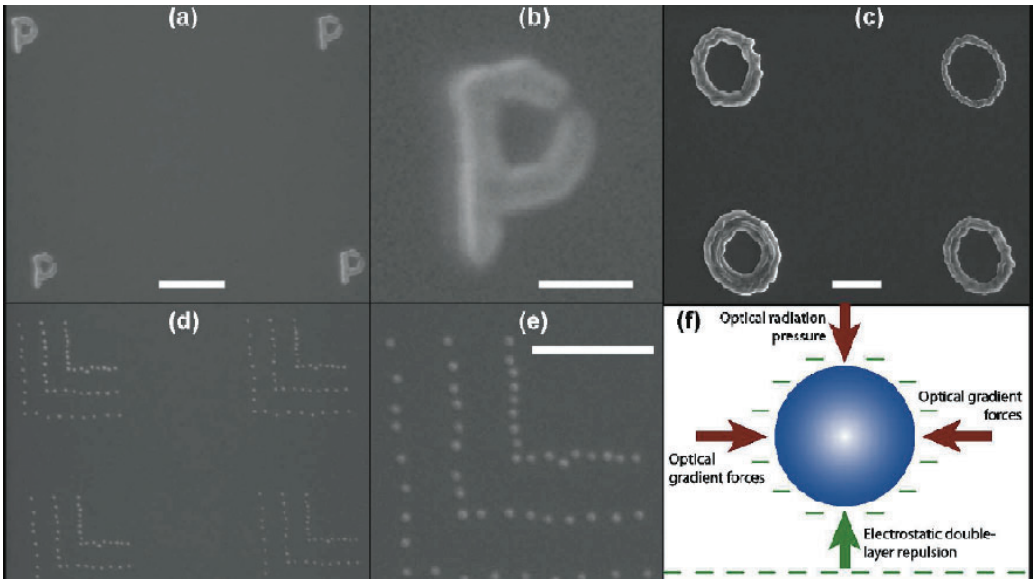

Figure 11 (online color at: www.lpr-journal.org) SEM images illustrating the ability to parallel processing using OTAN. (a) Four P's written using overlapping laser pulses with10 mJ/cm^2 incident fluence. (b) Overlaid image of the four P's in (a). (c) Four O's written using 12 mJ/cm^2 fluence, and particles of different sizes (0.75 µm upper-right, 3 µm lower-right, 2 µm the other two). This illustrates the capability to simultaneously produce different line widths in an array. (d) Four test patterns of individual shots used to test positioning accuracy and feature size uniformity (incident fluence is 15 mJ/cm^2). (e) The overlaid image of the four patterns in (d), illustrating the identical nature of the patterns. (f) Forces acting on the microsphere that maintain its position relative to the substrate without any feedback control. The scale bar in (b) is 500 nm, all other scale bars are 2 mm long [123].

and nanostructures [126, 127]. In this technique, a laser beam is scanned along a liquid photoresist to induce cross-linking. After exposure, the photoresist is developed, leading to microstructures in the areas the photoresist was exposed. Traditionally, polymerization has been performed with CW ultraviolet lasers over surfaces, which results in 2D structures [128]. More recently, complex 3D structures have been obtained with CW [129, 130] and picosecond lasers [131] by confining the photopolymerized region to the beam focal volume and then moving it with respect to the sample. This approach makes use of the threshold behavior of photoresists, which prevents any modification below a certain optical intensity. Alternatively, ultrafast lasers, taking advantage of multiphoton absorption, have been employed for photopolymerization [132]. In this case, the material modification can be much easily confined within the focal volume of the beam. Once again, by controlling the intensity of the Gaussian beam, the non-linear absorption allows one to overcome the diffraction limit [133] and produce structures with a nanometer resolution [134, 135].

The use of non-conventional beam shapes confers some benefits in photopolymerization as well. Again, the long depth of field of Bessel beams can be used to fabricate long structures without the need to translate a sample. This has been demonstrated through the fabrication of homogeneous polymer fibers using a CW laser with a Bessel beam [136]. Fibers as long as 15 mm, with a diameter below 5 µm (Fig. 12) have been fabricated through this approach. The length of the fiber greatly exceeded the maximal propagation distance that a Bessel beam should attain within the fluid used, due to waveguiding provided by the fiber

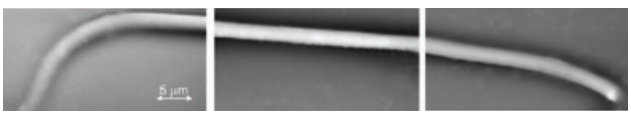

Figure 12 ESEM images of the left (a), middle (b) and right (c) parts of a polymer fiber with a length of 15 mm. The fiber was created illuminating a liquid photopolymer with a Bessel beam from a CW laser [136].

itself as it formed, a structure termed "self-written waveguide" [137]. Bessel beams have also been employed in the fabrication of 3D structures using multiphoton polymerization and scanning the beam through the volume of the sample [138, 139].

Annular beams can be used with polymerization to directly generate circles and related structures without the need for translation stages and their related problems [58, 140]. Moreover, translating the sample in the three directions of space in a step-and-repeat way allowed the annular patterns to be stacked into larger structures, as presented in Fig. 13.

Another important application of annular beams in photopolymerization is to enhance the resolution to sub 50 nm. Analogous to the STED microscopy technique [64], an annular beam used to deactivate the polymerization can be overlapped with a Gaussian beam that induces polymerization. Thus, the effective polymerization voxel would be confined in the center of the annulus. Reducing the dimensions of the annular center results in a smaller spot by further limiting the polymerization reaction above and beyond the

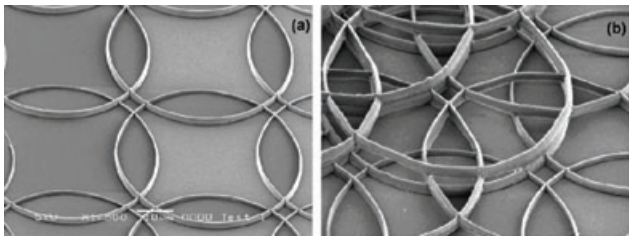

Figure 13 SEM images of complex patterns generated by 2 photon polymerization using an annular beam. The irradiated material had a low absorption cross section at the laser wavelength, and only at the focal region the beam intensity was high enough to produce photopolymerization through non-linear absorption processes. Translating the laser beam allowed the formation of (a) 2D and (b) 3D structures [138].

multiphoton effects. The combination of initiation and deactivation beams in polymerization has already demonstrated a resolution in the direction of the incident beam of $\lambda/20$ and further refinement continues to push the feature size smaller [141, 142].

4. Conclusions and outlook

We have presented a review of recent work in the processing of materials using Bessel and annular beams, as well as a discussion of the properties and generation methods for such structured illumination. Considering these aspects, it can be concluded that the use of shaped beams can be a scientifically interesting and technologically relevant alternative to conventional Gaussian and Top-hat beams for many applications. For instance, the "non-diffracting" behavior of Bessel beams results in a long depth of field, which can be used to increase the tolerance of the focal plane position during material processing. This allows the creation of uniform features over non-planar or uneven surfaces without the need to adjust the relative position of the sample and focus as with shorter depth of field beams. Such long depth of field also makes Bessel beams suitable to produce high aspect ratio structures, such as long channels in transparent materials or polymerized fibers, without scanning the beam inside the material or otherwise translating the sample. Similarly, annular beams have advantages for creating novel structures in materials, improved micromachining and deep-hole drilling, and reducing the feature size in multiphoton polymerization. Furthermore, the related vortex beams can induce unique light-matter interactions leading to enhanced ablative processing.

The role of laser beam shaping for scientific and industrial applications is expanding, increasing the breadth and capabilities of laser based materials processing. Novel and cost-effective methods to generate these structured beams have opened a new chapter in fundamental laser-matter interactions, enabling unique material responses with control down to the nanoscale, and have the potential to revolutionize the way lasers are used for processing. As we learn more about structured optical fields, their effect on materials, and new methods to tailor light properties, interesting possibilities will continue to emerge, providing fruitful opportunities for process development and optimization.

Acknowledgements. The authors acknowledge financial support from AFOSR and NSF, as well as useful conversations with Dr. M. Brown, Dr. S. Ramachandran, and Dr. A. Rode on aspects of this manuscript.

Received: 21 June 2011, **Revised:** 23 August 2011, **Accepted:** 5 October 2011

Published online: 17 January 2012

Key words: Bessel beam, annular beam, optical vortex, materials processing, nanopatterning, photopolymerization, non-diffracting beam.

Marti Duocastella studied physics at the University of Barcelona, where he obtained his Ph. D. in physics in 2010 on the study of the fundamentals of a laser printing technique for the fabrication of biosensors. He is currently a postdoctoral fellow at Princeton University. His current research involves the study of adaptive optics systems for laser processing and imaging applications.

Craig B. Arnold is an associate professor at Princeton University in the department of Mechanical and Aerospace Engineering and the Princeton Institute for Science and Technology of Materials (PRISM). His research interests involves laser processing and transport in materials with particular efforts in adaptive optics, laser based nanopatterning, and laser direct write technologies. He currently serves as the Associate Academic Director of PRISM and as the Princeton IGERT Director on Nanotechnology for Clean Energy.

References

[1] J. Wilson and J. F. B. Hawkes (eds.), Laser principles and applications (Prentice Hall International, Hertfordshire, UK, 1987).

[2] M. Brown and C. B. Arnold, in: Laser precision microfabrication, edited by K. Sugioka, M. Meunier, and A. Piqué (Springer-Verlag, Berlin, 2010).

[3] W. M. Steen (ed.), Laser Materials Processing (Springer, London, 1991).

[4] S. P. H. Narendra and B. Dahotre (eds.), Laser fabrication and machining of materials (Springer, New York, NY, 2008).

[5] W. Dudley (ed.), Laser Processing and Analysis of Materials (Plenum Press, New York, USA, 1983).

[6] E. Kannatey-Asibu (ed.), Principles of Laser Materials Processing (John Wiley & Sons, Inc., Hoboken, New Jersey, 2009).
[7] C. P. Grigoropoulos, S.-J. Moon, and M.-H. Lee, in: Laser Crystallization of Silicon-Fundamentals to Devices, edited by N. H. Nickel (Elsevier, Berlin, Germany, 2003), Chap. 2.
[8] G. Olivié, D. Giguère, F. Vidal, T. Ozaki, J. C. Kieffer, O. Nada, and I. Brunette, Opt. Express **16**, 4121 (2008).
[9] C. Hnatovsky, V. Shvedov, W. Krolikowski, and A. Rode, Phys. Rev. Lett. **106**, 123901 (2011).
[10] V. G. Niziev and A. V. Nesterov, J. Phys. D, Appl. Phys. **32**, 1455 (1999).
[11] J. P. Colombier, P. Combis, A. Rosenfeld, I. V. Hertel, E. Audouard, and R. Stoian, Phy. Rev. B **74**, 224106 (2006).
[12] B. N. Chichkov, C. Momma, S. Nolte, F. v. Alvensleben, and A. Tünnermann, Appl. Phys. A, Mater. **63**, 109 (1996).
[13] F. M. Dickey and S. C. Holswade (eds.), Laser beam shaping, theory and techniques (Marcel Dekker, New York, NY, 2000).
[14] R. Paschotta (ed.), Encyclopedia of laser physics and technology (Wiley-VCH, Weinheim; Chichester, 2008).
[15] K. Venkatakrishnan, B. Tan, L. H. K. Koh, and B. K. A. Ngoi, Opt. Laser Eng. **38**, 425 (2002).
[16] J. C. Ion (ed.), Laser processing of engineering materials: principles, procedure, and industrial application (Elsevier-Butterworth-Heinemann, Burlington, MA, 2005).
[17] A. E. Siegman (ed.), Lasers (University Science Books, Mill Valley, CA, 1986).
[18] H. Helvajian, in: Direct-write technologies for rapid prototyping applications, edited by A. Piqué and D. B. Chriesy (Academic Press, San Diego, CA, 2002), Chap. 14.
[19] M. Miyasaka and J. Stoemenos, J. Appl. Phys. **86**, 5556 (1999).
[20] D. B. Chrisey and G. K. Hubler (eds.), Pulsed laser deposition of thin films (J. Wiley, New York, 1994).
[21] K. Washio, in: Laser precision microfabrication, edited by K. Sugioka, M. Meunier, and A. Piqué (Springer-Verlag, Berlin, 2010), Chap. 3.
[22] K. Jain (ed.), Excimer laser lithography (SPIE Optical Engineering Press, Bellingham, Wash., USA, 1990).
[23] A. Masters and T. Geuking, Laser focus world **41** (2005).
[24] C. B. Arnold, P. Serra, and A. Pique, Mrs Bulletin **32**, 23 (2007).
[25] M. Colina, M. Duocastella, J. M. Fernandez-Pradas, P. Serra, and J. L. Morenza, J. Appl. Phys. **99** (2006).
[26] M. S. Brown, N. T. Kattamis, and C. B. Arnold, J. Appl. Phys. **107** (2010).
[27] R. Auyeung, H. Kim, N. Charipar, A. Birnbaum, S. Mathews, and A. Piqué, Appl. Phys. A, Mater., DOI: 10.1007/s00339 (2010).
[28] V. Garces-Chavez, D. McGloin, H. Melville, W. Sibbett, and K. Dholakia, Nature **419**, 145 (2002).
[29] K. Dholakia and W. M. Lee, in: Advances in Atomic, Molecular, and Optical Physics, Vol. 56, edited by E. Arimondo, P. R. Berman, and C. C. Lin (Academic Press, Burlington, MA, 2008), pp. 261–337.
[30] V. G. Shvedov, A. V. Rode, Y. V. Izdebskaya, A. S. Desyatnikov, W. Krolikowski, and Y. S. Kivshar, Phys. Rev. Lett. **105**, 118103 (2010).
[31] J. Arlt, T. Hitomi, and K. Dholakia, Appl. Phys. B, Laser O. **71**, 549 (2000).
[32] M. Padgett, J. Courtial, and L. Allen, Phys. Today **57**, 35 (2004).
[33] G. Molina-Terriza, J. P. Torres, and L. Torner, Nat. Phys. **3**, 305 (2007).
[34] M. Mazilu, D. Stevenson, F. Gunn-Moore, and K. Dholakia, Laser Photonics Rev. **4**, 529 (2010).
[35] N. Blow, Nature **456**, 825 (2008).
[36] S. W. Hell, Nat. Methods **6**, 24 (2009).
[37] X. Tsampoula, V. Garces-Chavez, M. Comrie, D. J. Stevenson, B. Agate, C. T. A. Brown, F. Gunn-Moore, and K. Dholakia, Appl. Phys. Lett. **91**, 053902 (2007).
[38] X. Tsampoula, K. Taguchi, T. Cizmár, V. Garces-Chavez, N. Ma, S. Mohanty, K. Mohanty, F. Gunn-Moore, and K. Dholakia, Opt. Express **16**, 17007 (2008).
[39] D. McGloin and K. Dholakia, Contemp. Phys. **46**, 15 (2005).
[40] L. Allen, M. W. Beijersbergen, R. J. C. Spreeuw, and J. P. Woerdman, Phys. Rev. A **45**, 8185 (1992).
[41] A. Bekshaev, K. Y. Bliokh, and M. Soskin, J. Opt. **13**, 053001 (2011).
[42] D. L. Andrews (ed.), Structured light and its applications (Elsevier: Academic Press, Amsterdam, 2008).
[43] T. Watanabe, M. Fujii, Y. Watanabe, N. Toyama, and Y. Iketaki, Rev. Sci. Instrum. **75**, 5131 (2004).
[44] D. Ganic, X. Gan, M. Gu, M. Hain, S. Somalingam, S. Stankovic, and T. Tschudi, Opt. Lett. **27**, 1351 (2002).
[45] D. Zeng, W. P. Latham, and A. Kar, J. Laser Appl. **17**, 256 (2005).
[46] J. Durnin, J. J. Miceli, and J. H. Eberly, Phys. Rev. Lett. **66**, 838 (1991).
[47] P. Polesana, D. Faccio, P. Di Trapani, A. Dubietis, A. Piskarskas, A. Couairon, and M. A. Porras, Opt. Express **13**, 6160 (2005).
[48] J. Durnin, J. J. Miceli, and J. H. Eberly, Phys. Rev. Lett. **58**, 1499 (1987).
[49] M. A. Sheikh and L. Li, P. I. Mech. Eng. C, J. Mec. **224**, 1061 (2010).
[50] C. Hnatovsky, V. G. Shvedov, W. Krolikowski, and A. V. Rode, Opt. Lett. **35**, 3417 (2010).
[51] S. Safdar, L. Li, M. A. Sheikh, and L. Zhu, Opt. Laser Technol. **39**, 1101 (2007).
[52] J. W. Goodman (ed.), Introduction to Fourier optics (Roberts, Englewood, Colorado, 2005).
[53] J. H. McLeod, J. Opt. Soc. Am. **44**, 592 (1954).
[54] G. Roy and R. Tremblay, Opt. Commun. **34**, 1 (1980).
[55] I. Alexeev, K. H. Leitz, A. Otto, and M. Schmidt, Phys. Procedia **5**, 533 (2010).
[56] Y. Matsuoka, Y. Kizuka, and T. Inoue, Appl. Phys. A, Mater. **84**, 423 (2006).
[57] M. Rioux, R. Tremblay, and P. A. Belanger, Appl. Opt. **17**, 1532 (1978).
[58] R. J. Winfield, B. Bhuian, S. O'Brien, and G. M. Crean, Appl. Phys. Lett. **90**, 111115 (2007).
[59] G. Milne, G. D. M. Jeffries, and D. T. Chiu, Appl. Phys. Lett. **92**, 261101 (2008).
[60] J. Amako, K. Yoshimura, D. Sawaki, and T. Shimoda, Proceedings SPIE **5713**, 497 (2005).
[61] U. Efron (ed.), Spatial light modulator technology: materials, devices, and applications (Marcel Dekker, New York, 1995).
[62] C. Maurer, A. Jesacher, S. Bernet, and M. Ritsch-Marte, Laser Photonics Rev. **5**, 81 (2011).
[63] F. Courvoisier, P. A. Lacourt, M. Jacquot, M. K. Bhuyan, L. Furfaro, and J. M. Dudley, Opt. Lett. **34**, 3163 (2009).

[64] K. I. Willig, B. Harke, R. Medda, and S. W. Hell, Nat Meth **4**, 915 (2007).
[65] J. A. Davis, E. Carcole, and D. M. Cottrell, Appl. Opt. **35**, 599 (1996).
[66] A. M. Weiner, Rev. Sci. Instrum. **71**, 1929 (2000).
[67] R. J. Beck, J. P. Parry, W. N. MacPherson, A. Waddie, N. J. Weston, J. D. Shephard, and D. P. Hand, Opt. Express **18**, 17059 (2010).
[68] E. McLeod, A. B. Hopkins, and C. B. Arnold, Opt. Lett. **31**, 3155 (2006).
[69] K. A. Higginson, M. A. Costolo, and E. A. Rietman, Appl. Phys. Lett. **84**, 843 (2004).
[70] C. B. Arnold and E. McLeod, Photon. Spectra **41**, 78 (2007).
[71] E. McLeod and C. B. Arnold, J. Appl. Phys. **102**, 033104:1–9 (2007).
[72] E. McLeod and C. B. Arnold, Appl. Opt. **47**, 3609 (2008).
[73] A. Mermillod-Blondin, E. McLeod, and C. B. Arnold, Opt. Lett. **33**, 2146 (2008).
[74] N. Olivier, A. Mermillod-Blondin, C. B. Arnold, and E. Beaurepaire, Opt. Lett. **34**, 1684 (2009).
[75] A. Mermillod-Blondin, E. McLeod, and C. B. Arnold, Appl. Phys. A, Mater. **93**, 231 (2008).
[76] M. Duocastella and C. B. Arnold, to be published (2011).
[77] F. W. Wise, A. Chong, and W. H. Renninger, Laser Photonics Rev. **2**, 58 (2008).
[78] S.-K. Eah, W. Jhe, and Y. Arakawa, Rev.Sci. Instr. **74**, 4969 (2003).
[79] K. M. Tan, M. Mazilu, T. H. Chow, W. M. Lee, K. Taguchi, B. K. Ng, W. Sibbett, C. S. Herrington, C. T. A. Brown, and K. Dholakia, Opt. Express **17**, 2375 (2009).
[80] T. Grosjean, S. S. Saleh, M. A. Suarez, I. A. Ibrahim, V. Piquerey, D. Charraut, and P. Sandoz, Appl. Opt. **46**, 8061 (2007).
[81] J. K. Kim, J. Kim, Y. Jung, W. Ha, Y. S. Jeong, S. Lee, A. Tünnermann, and K. Oh, Opt. Lett. **34**, 2973 (2009).
[82] X. Zhu, A. Schulzgen, L. Li, and N. Peyghambarian, Appl. Phys. Lett. **94**, 201102 (2009).
[83] S. R. Lee, J. Kim, S. Lee, Y. Jung, J. K. Kim, and K. Oh, Opt. Express **18**, 25299 (2010).
[84] S. Ramachandran, J. W. Nicholson, S. Ghalmi, M. F. Yan, P. Wisk, E. Monberg, and F. V. Dimarcello, Opt. Lett. **31**, 1797 (2006).
[85] S. Ramachandran, J. M. Fini, M. Mermelstein, J. W. Nicholson, S. Ghalmi, and M. F. Yan, Laser Photonics Rev. **2**, 429 (2008).
[86] R. Siddharth and G. Samir, in: Proceedings of the Conference on Lasers and Electro-Optics/Quantum Electronics and Laser Science Conference and Photonic Applications Systems Technologies (Optical Society of America, San Jose, CA, 2008), paper CPDB5.
[87] J. Yin, H.-R. Noh, K.-I. Lee, K.-H. Kim, Y.-Z. Wang, and W. Jhe, Opt. Commun. **138**, 287 (1997).
[88] H. Ma, H. Cheng, W. Zhang, L. Liu, and Y. Wang, Chin. Opt. Lett. **5**, 460 (2007).
[89] C. Zhao, Y. Cai, F. Wang, X. Lu, and Y. Wang, Opt. Lett. **33**, 1389 (2008).
[90] A. Vasara, J. Turunen, and A. T. Friberg, J. Opt. Soc. Am. A **6**, 1748 (1989).
[91] W.-X. Cong, N.-X. Chen, and B.-Y. Gu, J. Opt. Soc. Am. A **15**, 2362 (1998).
[92] T. A. Klar, S. Jakobs, M. Dyba, A. Egner, and S. W. Hell, Proc. Natl. Acad. Sci. USA **97**, 8206 (2000).
[93] K. Sueda, G. Miyaji, N. Miyanaga, and M. Nakatsuka, Opt. Express **12**, 3548 (2004).
[94] V. G. Shvedov, C. Hnatovsky, W. Krolikowski, and A. V. Rode, Opt. Lett. **35**, 2660 (2010).
[95] O. Suttmann, A. Moalem, R. Kling, and A. Ostendorf, in: Laser precision microfabrication, edited by K. Sugioka, M. Meunier, and A. Piqué (Springer-Verlag, Berlin, 2010), Chap. 13.
[96] N. Sanner, N. Huot, E. Audouard, C. Larat, and J. P. Huignard, Opt. Laser Eng. **45**, 737 (2007).
[97] D. Zeng, W. P. Latham, and A. Kar, Proceedings of SPIE **6290**, 62900J (2006).
[98] A. Mermillod-Blondin, E. McLeod, and C. B. Arnold, Appl. Phys. A, Mater. **93**, 231 (2008).
[99] M. Kohno and Y. Matsuoka, JSME. Int. J. B, Fluid. T. **47**, 497 (2004).
[100] R. Grunwald, U. Neumann, A. Rosenfeld, J. Li, and P. R. Herman, Opt. Lett. **31**, 1666 (2006).
[101] R. R. Gattass and E. Mazur, Nat. Photon. **2**, 219 (2008).
[102] A. Couairon and A. Mysyrowicz, Phys. Rep. **441**, 47 (2007).
[103] Y. Hayasaki, M. Isaka, A. Takita, and S. Juodkazis, Opt. Express **19**, 5725 (2011).
[104] A. Marcinkevicius, S. Juodkazis, S. Matsuo, V. Mizeikis, and H. Misawa, Jpn. J. Appl. Phys. 2 **40**, L1197 (2001).
[105] J. Amako, D. Sawaki, and E. Fujii, J. Opt. Soc. Am. B, Opt. Phys. **20**, 2562 (2003).
[106] Z. Veronique, M. Nathalie, and P. Michel, Proceedings SPIE **7099**, 70992J (2008).
[107] Z. Veronique, M. Nathalie, and P. Michel, Proceedings SPIE **7386**, 738632 (2009).
[108] M. K. Bhuyan, F. Courvoisier, P. A. Lacourt, M. Jacquot, L. Furfaro, M. J. Withford, and J. M. Dudley, Opt. Express **18**, 566 (2010).
[109] E. Gaizauskas, E. Vanagas, V. Jarutis, S. Juodkazis, V. Mizeikis, and H. Misawa, Opt. Lett. **31**, 80 (2006).
[110] P. Polesana, M. Franco, A. Couairon, D. Faccio, and P. Di Trapani, Phys. Rev. A **77**, 043814 (2008).
[111] M. K. Bhuyan, F. Courvoisier, P. A. Lacourt, M. Jacquot, R. Salut, L. Furfaro, and J. M. Dudley, Appl. Phys. Lett. **97**, 081102 (2010).
[112] J. Hamazaki, R. Morita, K. Chujo, Y. Kobayashi, S. Tanda, and T. Omatsu, Opt. Express **18**, 2144 (2010).
[113] D. Appell, Nature **419**, 553 (2002).
[114] M. C. Roco, Curr. Opin. Biotechnol. **14**, 337 (2003).
[115] E. Betzig and J. K. Trautman, Science **257**, 189 (1992).
[116] S. M. Huang, M. H. Hong, B. Lukiyanchuk, and T. C. Chong, Appl. Phys. A, Mater. **77**, 293 (2003).
[117] Y. Hsiharng, C.-K. Chao, M.-K. Wei, and C.-P. Lin, J. Micromech. Microeng. **14**, 1197 (2004).
[118] Y. Lin, M. H. Hong, T. C. Chong, C. S. Lim, G. X. Chen, L. S. Tan, Z. B. Wang, and L. P. Shi, Appl. Phys. Lett. **89**, 041108 (2006).
[119] Y. Zhou, M. H. Hong, J. Y. H. Fuh, L. Lu, and B. S. Luk, 'yanchuk, Z. B. Wang, L. P. Shi, and T. C. Chong, Appl. Phys. Lett. **88**, 023110 (2006).
[120] W. Wu, A. Katsnelson, O. G. Memis, and H. Mohseni, Nanotechnology **18**, 485302 (2007).
[121] E. McLeod and C. B. Arnold, Nat. Nanotechnol. **3**, 413 (2008).
[122] R. Fardel, E. McLeod, Y.-C. Tsai, and C. Arnold, Appl. Phys. A, Mater **101**, 41 (2010).
[123] E. McLeod and C. B. Arnold, Opt. Express **17**, 3640 (2009).

[124] Y.-C. Tsai, R. Fardel, and C. B. Arnold, AIP Conf. Proc. **1278**, 457 (2010).
[125] Y. C. Tsai, R. Fardel, and C. B. Arnold, Appl. Phys. Lett. **98**, 233110 (2011).
[126] R. Nassar and W. Dai (eds.), Modelling of microfabrication systems (Springer-Verlag, Berlin, 2003).
[127] S. Maruo and J. T. Fourkas, Laser Photonics Rev. **2**, 100 (2008).
[128] C. Decker, in: L. F. Thompson, C. G. Willson, and J. M. J. Fréchet (eds.), Materials for Microlithography Radiation-Sensitive Polymers (American Chemical Society, Washington, 1985), Chap. 9.
[129] S. Maruo and K. Ikuta, Appl. Phys. Lett. **76**, 2656 (2000).
[130] M. Thiel, J. Fischer, G. v. Freymann, and M. Wegener, Appl. Phys. Lett. **97**, 221102 (2010).
[131] M. Malinauskas, P. Danilevicius, and S. Juodkazis, Opt. Express **19**, 5602 (2011).
[132] S. Maruo, O. Nakamura, and S. Kawata, Opt. Lett. **22**, 132 (1997).
[133] S. Kawata, H.-B. Sun, T. Tanaka, and K. Takada, Nature **412**, 697 (2001).
[134] L. Li, E. Gershgoren, G. Kumi, W.-Y. Chen, P. T. Ho, W. N. Herman, and J. T. Fourkas, Adv. Mater. **20**, 3668 (2008).
[135] M. Farsari and B. N. Chichkov, Nat Photon **3**, 450 (2009).
[136] J. Jezek, T. Cizmár, V. Nedela, and P. Zemánek, Opt. Express **14**, 8506 (2006).
[137] S. J. Frisken, Opt. Lett. **18**, 1035 (1993).
[138] X. F. Li, R. J. Winfield, S. O'Brien, and G. M. Crean, Appl. Surf. Sci. **255**, 5146 (2009).
[139] C. F. Phelan, R. J. Winfield, D. P. O'Dwyer, Y. P. Rakovich, J. F. Donegan, and J. G. Lunney, Opt. Commun. **284**, 3571 (2011).
[140] B. Bhuian, R. J. Winfield, S. O'Brien, and G. M. Crean, Appl. Surf. Sci. **254**, 841 (2007).
[141] L. Li, R. R. Gattass, E. Gershgoren, H. Hwang, and J. T. Fourkas, Science **324**, 910 (2009).
[142] M. P. Stocker, L. Li, R. R. Gattass, and J. T. Fourkas, Nat. Chem. **3**, 223 (2011).